




## Article

# Transcription Factor *Mavib-1* Negatively Regulates Conidiation by Affecting Utilization of Carbon and Nitrogen Source in *Metarhizium acridum*

Xueling Su <sup>1,2,3</sup> , Hong Liu <sup>1,2,3</sup>, Yuxian Xia <sup>1,2,3,\*</sup>  and Yueqing Cao <sup>1,2,3,\*</sup> 

<sup>1</sup> School of Life Sciences, Chongqing University, Chongqing 401331, China; xuelingsu@haut.edu.cn (X.S.); 202126021033@cqu.edu.cn (H.L.)

<sup>2</sup> Chongqing Engineering Research Center for Fungal Insecticides, Chongqing 401331, China

<sup>3</sup> Key Laboratory of Gene Function and Regulation Technologies under Chongqing Municipal Education Commission, Chongqing 401331, China

\* Correspondence: yuxianxia@cqu.edu.cn (Y.X.); yueqingcao@cqu.edu.cn (Y.C.)

**Abstract:** Conidium is the main infection unit and reproductive unit of pathogenic fungi. Exploring the mechanism of conidiation and its regulation contributes to understanding the pathogenicity of pathogenic fungi. *Vib-1*, a transcription factor, was reported to participate in the conidiation process. However, the regulation mechanism of *Vib-1* in conidiation is still unclear. In this study, we analyzed the function of *Vib-1* and its regulation mechanism in conidiation through knocking out and overexpression of *Vib-1* in entomopathogenic fungus *Metarhizium acridum*. Results showed that the colonial growth of *Mavib-1* disruption mutant ( $\Delta Mavib-1$ ) was significantly decreased, and conidiation was earlier compared to wild type (WT), while overexpression of *Mavib-1* led to a delayed conidiation especially when carbon or nitrogen sources were insufficient. Overexpression of *Mavib-1* resulted in a conidiation pattern shift from microcycle conidiation to normal conidiation on nutrient-limited medium. These results indicated that *Mavib-1* acted as a positive regulator in vegetative growth and a negative regulator in conidiation by affecting utilization of carbon and nitrogen sources in *M. acridum*. Transcription profile analysis demonstrated that many genes related to carbon and nitrogen source metabolisms were differentially expressed in  $\Delta Mavib-1$  and OE strains compared to WT. Moreover, *Mavib-1* affects the conidial germination, tolerance to UV-B and heat stresses, cell wall integrity, conidial surface morphology and conidial hydrophobicity in *M. acridum*. These findings unravel the regulatory mechanism of *Mavib-1* in fungal growth and conidiation, and enrich the knowledge to conidiation pattern shift of filamentous fungi.



**Citation:** Su, X.; Liu, H.; Xia, Y.; Cao, Y. Transcription Factor *Mavib-1* Negatively Regulates Conidiation by Affecting Utilization of Carbon and Nitrogen Source in *Metarhizium acridum*. *J. Fungi* **2022**, *8*, 594. <https://doi.org/10.3390/jof8060594>

Academic Editor: Ulrich Kück

Received: 30 April 2022

Accepted: 29 May 2022

Published: 1 June 2022

**Publisher's Note:** MDPI stays neutral with regard to jurisdictional claims in published maps and institutional affiliations.



**Copyright:** © 2022 by the authors. Licensee MDPI, Basel, Switzerland. This article is an open access article distributed under the terms and conditions of the Creative Commons Attribution (CC BY) license (<https://creativecommons.org/licenses/by/4.0/>).

**Keywords:** entomopathogenic fungi; transcription factor *Mavib-1*; conidiation; carbon and nitrogen utilization

## 1. Introduction

The insect pathogenic fungi *Metarhizium* spp. and *Beauveria* spp. have been widely used all over the world and play an important role in the control of agricultural pests [1–7]. Representative species, such as *Metarhizium anisopliae*, *Metarhizium acridum* and *Beauveria bassiana*, have been developed as environmentally friendly biopesticides [8,9]. Entomopathogenic fungi mainly infect host insects through conidia, which are produced under complex regulation. Clarification of the regulation mechanisms of conidiation is also helpful for understanding their invasion and growth inside host insects.

Most fungi have two types of conidiation: normal conidiation (NC) and microcycle conidiation (MC) [10]. Normally, conidiophores arise from the vegetative mycelia and produce large amounts of conidia [11,12], which is the most common conidiation type for filamentous fungi [13]. The fungi can bypass the mycelia period in MC and develop secondary conidia from germ tubes or directly from conidial cells [1,4,14]. MC is

a special survival mechanism of fungi under adverse conditions, such as high temperature [10,11,15], extreme pH [16], high salt content [17], and nutritional deficiencies [4,18–20]. Among them, nutritional deficiency is the important factor that affects the fungal growth and development.

A previous investigation showed that *M. acridum* produces conidia by NC on nutrient-rich medium 1/4 SDAY (Sabouraud dextrose medium with yeast extract) and MC on the nutrient-deficient medium SYA (sucrose yeast extract agar) [4]. However, adding a single carbon source (sucrose) or nitrogen source (sodium nitrate) in SYA medium can make the *M. acridum* switch to the NC type, indicating that nutrient element plays important roles in the conidiation pattern shift in *M. acridum* [20]. The underlying regulation mechanisms of changes from conidiation to vegetative growth when nutrients are changed are still largely unknown. A *Vib-1* gene (vegetative incompatibility blocked) was highly upregulated when sucrose was added to SYA medium, indicating a possible role of *Vib-1* in conidiation and conidiation pattern shift by affecting the nutrient utilization in *M. acridum*.

*Vib-1* belongs to the Ndt80/PhoG DNA binding protein family and contains a conserved DNA-binding domain NDT80\_PhoG. In *Neurospora crassa*, *Vib-1* participates in the regulation of heterokaryotic incompatibility and conidiation [21], and also regulates the expression of cell wall-degrading enzymes (PCWDEs) [22]. *Vib-1* acts as a main regulator of the response to carbon and nitrogen starvation. Loss of *Vib-1* leads to the imbalance of Carbon Catabolite Repression (CCR), which inhibits glucose signaling and CCR under carbon-limited conditions in *N. crassa* [23]. In *Aspergillus nidulans*, *Vib-1* is required for production of extracellular proteases in response to carbon and nitrogen starvation [23,24]. However, the roles of *Vib-1* in entomopathogenic fungi and its regulation mechanism in conidiation and fungal growth are not clear.

On SYA medium, the change of nutrients can directly lead to a switch between vegetative growth and conidiation, that is, switching between MC and NC. Therefore, in this study, we used SYA medium to analyze the effect of *Mavib-1* on fungal development under different nutritional conditions in *M. acridum* through gene disruption and overexpression techniques. Exploring the function of transcription factor *Mavib-1* and its mechanism of conidiation pattern shift in *M. acridum* will help to further understand the molecular mechanism of nutrient-regulated fungal conidiation mode shift.

## 2. Materials and Methods

### 2.1. Fungal Strains and Growth Conditions

*M. acridum* CQMa102 was used as a wild-type strain (WT) and stored in the China General Microbiological Culture Collection Center (CGMCC, No. 0877, NCBI Assembly No. GCF\_000187405.1) [25]. The WT strain and transformants generated in this study were grown on 1/4 SDAY (1% dextrose; 0.25% peptone; 0.5% yeast extract and 2% agar) and incubated for 15 days at 28 °C. The influence of nutrient on conidiation was determined on SYA medium (sucrose 3%, yeast extract 0.5%, NaNO<sub>3</sub> 0.3%, K<sub>2</sub>HPO<sub>4</sub> 0.1%, MgSO<sub>4</sub>·7H<sub>2</sub>O 0.05%, KCl 0.05%, FeSO<sub>4</sub>·7H<sub>2</sub>O 0.001%, MnSO<sub>4</sub>·H<sub>2</sub>O 0.001% and agar 1.8%) or SYA with replaced sucrose by other carbon source. Dextrose, agar, NaNO<sub>3</sub>, MgSO<sub>4</sub>·7H<sub>2</sub>O and FeSO<sub>4</sub>·7H<sub>2</sub>O were purchased from Chengdu Kelon Chemical Co., Ltd. (Chengdu, China); yeast extract and peptone were purchased from Beijing Aoboxing Biotechnology Co., Ltd. (Beijing, China); sucrose was purchased from Sinopharm Chemical Reagent Co., Ltd. (Shanghai, China). All chemicals were purchased from Chongqing Chuandong Chemical Co., Ltd. (Chongqing, China) unless stated separately.

### 2.2. Deletion, Complementation and Overexpression of the *Mavib-1* Gene

The *Mavib-1* (Gene ID: MT954969) disruption mutant was constructed by homologous recombination. For *Mavib-1* deletion, upstream and downstream flanking fragments (~1 kb) of *Mavib-1* coding sequences were amplified and inserted into the pK2-PB vector which harbored a *bar* cassette. The resulting vector pK2-PB-*Mavib-1*-LR was transformed into *M. acridum* mediated by *Agrobacterium tumefaciens* [26]. The *Mavib-1* disruption mu-

tants ( $\Delta Mavib-1$ ) were screened on Czapek-Dox medium (sucrose 30 g/L,  $\text{NaNO}_3$  2 g/L,  $\text{KH}_2\text{PO}_4$  1 g/L,  $\text{MgSO}_4 \cdot 7\text{H}_2\text{O}$  0.5 g/L, KCl 0.5 g/L,  $\text{FeSO}_4 \cdot 7\text{H}_2\text{O}$  0.01 g/L and agar 18 g/L) containing 500  $\mu\text{g}/\text{mL}$  glufosinate-ammonium (Sigma, St. Louis, MO, USA). To rescue the deleted *Mavib-1*, the full-length *Mavib-1* sequence including flanking regions (5.0 kb in total length) was amplified and inserted into the pK2-*sur* vector containing the chlorimuron ethyl resistance gene *sur* [27] to construct the complementary vector pK2-*sur-Mavib-1*. This vector was transformed into  $\Delta Mavib-1$  and the complementary transformants (CP) were screened on Czapek-Dox plate containing 60  $\mu\text{g}/\text{mL}$  chlorimuron ethyl (Sigma, Bellefonte, PA, USA). To create an *Mavib-1* overexpression mutant, the *Mavib-1* gene was fused with *EGFP* and driven by the promotor of constitutive glyceraldehyde 3-phosphate dehydrogenase gene (*Magpd*). This vector was transformed into the WT and transformants (OE) were screened on Czapek-Dox plates supplemented with 500  $\mu\text{g}/\text{mL}$  glufosinate-ammonium (Sigma, St. Louis, MO, USA). The transformants were verified by PCR, and florescence was observed under a laser scanning confocal microscope (LSCM, TCS SP8, Leica, Germany).

### 2.3. Transcription Activation Experiment

For the transcriptional activation test, full-length cDNA, N-terminal (contain NDT80\_PhoG domain) and C-terminal of *Mavib-1* was amplified from a cDNA library with primer pairs *Mavib-1*-BD-F1/*Mavib-1*-BD-R2, *Mavib-1*-BD-F1/*Mavib-1*-BD-R1, *Mavib-1*-BD-F2/*Mavib-1*-BD-R2 (Table S1), respectively, and the amplified fragments were respectively inserted into the vector pBKT7 (Clontech) between the *NdeI* and *EcoRI* sites under the control of the GAL4 promoter to generate plasmid pBKT7-*Mavib-1* for transformation into the Yeast Y2H Gold strain. Putative prototrophic transformants were selected on a Trp-free SD medium and further transferred onto Trp/His/Ade-free SD plates containing 0.5 mM 5-Bromo-4-Chloro-3-Indolyl-D-Galactopyranoside (*X- $\alpha$ -gal*, TaKaRa, Dalian, China) for transcriptional activation assay.

### 2.4. Stress Tolerance Assays

For the stress assays, aliquots of 2  $\mu\text{L}$  conidial suspensions ( $1 \times 10^6$  conidia/mL) of the WT,  $\Delta Mavib-1$ , CP and OE strains were pipetted onto 1/4 SDAY plates supplemented with 1 mol/L NaCl, 0.01% SDS, 1 mol/L sorbitol (SOR) (Dingguo, Beijing, China), 500  $\mu\text{g}/\text{mL}$  Congo Red (CR) (Solarbio, Beijing, China), 6 mmol/L  $\text{H}_2\text{O}_2$ , 50  $\mu\text{g}/\text{mL}$  calcofluor white (CFW) (Solarbio, Beijing, China), respectively. The plates were incubated at 28 °C for 5 days. Stress tolerance to heat and ultraviolet radiation was assessed as described previously [4]. Half inhibition time of germination ( $\text{IT}_{50}$ ) under UV radiation or heat was then calculated for each strain. The assays were conducted with three replicates per treatment and the experiment was repeated three times.

### 2.5. Conidial Germination

Conidial germination assay was conducted on 1/4 SDAY plates as described previously [28]. The conidia of *M. acridum* WT,  $\Delta Mavib-1$ , CP and OE strains were suspended in sterile water ( $1 \times 10^7$ /mL). Aliquots of 50  $\mu\text{L}$  conidia suspension were spread on 1/4 SDAY plates and the plates were incubated at 28 °C. The conidial germination rate of each strain was determined every 2 h (cultured for 2, 4, 6, 8, 10 and 12 h, respectively) until conidia germinate almost completely. The half time to germination ( $\text{GT}_{50}$ ) was statistically calculated, and the data were analyzed. Three replicates in each independent experiment were conducted, and in each replicate, 300 conidia were used.

### 2.6. Electronic Microscopy

Ultrastructure of mature conidial cell wall surface of the WT,  $\Delta Mavib-1$ , CP and OE strains was examined by scanning electronic microscopy (SEM, SU8010, Hitachi, Japan) as described previously [29]. Conidia of WT,  $\Delta Mavib-1$ , CP and OE strains of *M. acridum* were collected, fixed with 2.5% glutaraldehyde solution (Servicebio, Wuhan, China) at 4 °C overnight, and then the samples were processed as follows: remove the fixation solution,

rinse the samples three times with 0.1 M phosphate buffer, pH 7.0, 15 min each time; fix the sample with 1% osmic acid solution for 1–2 h; carefully remove the osmic acid waste solution, rinse the sample three times with 0.1 M, pH 7.0 phosphate buffer for 15 min each time; use a gradient concentration (including 30%, 50%, 70%, 80%, 90% and 95%) ethanol solution to dehydrate the samples with each concentration for 15 min, and then treated with 100% ethanol twice, each time for 20 min. Rinse the sample with a mixture of ethanol and isoamyl acetate ( $v/v = 1/1$ ) for 30 min, and then rinse with pure isoamyl acetate for 1h or leave the samples overnight. After critical point drying and coating, the samples were observed in a scanning electron microscope.

### 2.7. Conidial Hydrophobicity Assay

Conidial hydrophobicity was determined with hexadecane as described previously [29]. Conidia of WT,  $\Delta Mavib-1$ , CP and OE strains were suspended ( $3 \times 10^7$  conidia/mL) in reaction buffer (22.2 g/L  $K_2HPO_4$ , 7.26 g/L  $KH_2PO_4$ , 1.8 g/L urea, 0.2 g/L  $MgSO_4$ , pH 7.1). Aliquots of 1 mL conidia suspension ( $OD_{470} = 0.4$ ) were mixed well with 100  $\mu$ L hexadecane and then incubated at 25 °C for 10 min. The upper hexadecane was discarded. The absorption peak of conidia suspension at 470 nm ( $A_{470}$ ) was measured after removing solidified hexadecane completely after incubation at 4 °C for 30 min. The hydrophobic index was calculated using the following formula:  $(A_{470, \text{control}} - A_{470, \text{hexadecane-treated}}) / (A_{470, \text{control}})$ . The assays were conducted with three replicates per treatment and the experiment was repeated three times.

### 2.8. Conidiation and Colony Morphology with Various Carbon or Nitrogen Sources

SYA containing different carbon sources at 3% ( $w/v$ ) (glucose, sucrose and glycerol, respectively) or SYA containing different nitrogen sources at 3% ( $w/v$ ) (urea, glutamine/Gln,  $NaNO_3$ , respectively) were used for colony growth assays and conidiation analysis. For conidiation observation under microscope, each plate was spread evenly with 100  $\mu$ L of conidial suspension ( $1 \times 10^7$  conidia/mL) and incubated at 28 °C for 12–36 h. For colony growth assay, aliquots of 2  $\mu$ L of conidial suspension ( $1 \times 10^6$  conidia/mL) of each strain were inoculated on different media and the plates were incubated at 28 °C for 5 days. For conidial yield assay, 2  $\mu$ L conidial suspensions ( $1 \times 10^6$  conidia/mL) of WT,  $\Delta Mavib-1$ , CP and OE were spotted onto  $\frac{1}{4}$  SDAY medium in a 24-hole plate and incubated at 28 °C. Conidia were collected after growing for 15 days and vortexed with 1 mL of 0.05% Tween 80. Conidial concentration was determined using a hemocytometer under a microscope. All experiments were performed three times.

### 2.9. RNA-Seq

Transcriptional profiles were measured in WT,  $\Delta mavib-1$  and OE strains by RNA-Seq. Total RNA was extracted from WT,  $\Delta mavib-1$ , or OE strains after growing on SYA plates at 28 °C for 20 h. Total RNA was extracted from each sample using an RNA Kit (Invitrogen, Carlsbad, CA, USA) with Rnase-free DnaseI added and reverse transcribed into cDNA with an oligo-dT primer using the PrimeScript RT Master Mix (TaKaRa, Dalian, China). Sequencing libraries were prepared, and sequencing was conducted on BGISEQ-500 (BGI, Beijing, China). Genes were classed as significantly differentially expressed when false discovery rate (FDR)  $< 0.001$  and fold change  $\geq 2$ .

Differentially expressed genes (DEGs) were classified and annotated using gene ontology (GO) and Kyoto Encyclopedia of Genes and Genomes (KEGG) pathway analysis.

### 2.10. Reverse Transcription Quantitative PCR (RT-qPCR)

The gene expression levels were examined by RT-qPCR. Amplification mixtures (20  $\mu$ L) contained 1  $\mu$ L template cDNA, 10  $\mu$ L IQ SYBR Green Supermix (2 $\times$ , Bio-Rad, Foster City, CA, USA) and 1  $\mu$ L of each primer (qF/qR, 10  $\mu$ mol/L) [27]. The reactions were performed in iCycler system (Bio-Rad). The *Magpd* gene (EFY84384), amplified with primers gpd-F/gpd-R (Table S1), was used as the endogenous control, as described previously [27].



Transcript ratios of the target gene were evaluated using the  $2^{-\Delta\Delta CT}$  method [30]. All PCR amplifications were conducted in triplicate, and trials were repeated three times.

### 2.11. Data Analysis

All measurements were analyzed using a one-way ANOVA model with the SPSS 19.0 program (SPSS Inc., Chicago, IL, USA). Tukey's honestly significant difference test was used to evaluate means at  $\alpha = 0.05$ .

## 3. Results

### 3.1. Structural Features and Deletion of *Mavib-1*

*Mavib-1* gene has a full-length sequence of 1991 bp containing two introns (67 bp and 79 bp). A cDNA sequence of 1845 bp (Acc. MT954969) encodes a protein of 614 amino acids with a molecular weight of 66.90 kDa and an isoelectric point of 6.84. The *Mavib-1* protein contains an NDT80\_PhoG domain with 165 amino acids (Residues 171–335) (Figure S1A), which is highly conserved in *Vib-1* homologs among different fungi (Figure S1B). Phylogenetic analysis revealed that *Mavib-1* was clustered with other fungal NDT80\_PhoG domain containing proteins (Figure S1C). To elucidate the functions of *Mavib-1* in *M. acridum*,  $\Delta$ *Mavib-1*, CP and OE strains were constructed (Figure S2A), and the expected recombinant events were verified by PCR (Figure S2B), Semi-quantitative RT-PCR (Figure S2C) and RT-qPCR analysis (Figure S2D).

### 3.2. C-Terminal of *Mavib-1* Has Transactivation Activity

*Mavib-1-N* (containing NDT80 domain), *Mavib-1-C* or *Mavib-1* full CDS were fused to the GAL4 DNA-binding domain and expressed in yeast strain Y2H Gold. *Mavib-1-C* fusion strain showed blue spots on SD-Trp plates containing X- $\alpha$ -gal and AbA, indicating a transactivation activity at C-terminal of *Mavib-1* in yeast (Figure 1A). To investigate the subcellular localization of *Mavib-1*, *Mavib-EGFP* was expressed in *M. acridum*. Results showed that green fluorescent signal was observed in the nucleus in both conidia and mycelia and overlapped with the staining of DAPI dye, indicating a nuclear localization of *Mavib-1* (Figure 1B). Therefore, consistent with *Vib-1* in *A. nidulans* and *N. crassa* [22,23], *Mavib-1* can functionally act as a transcription factor in *M. acridum*.

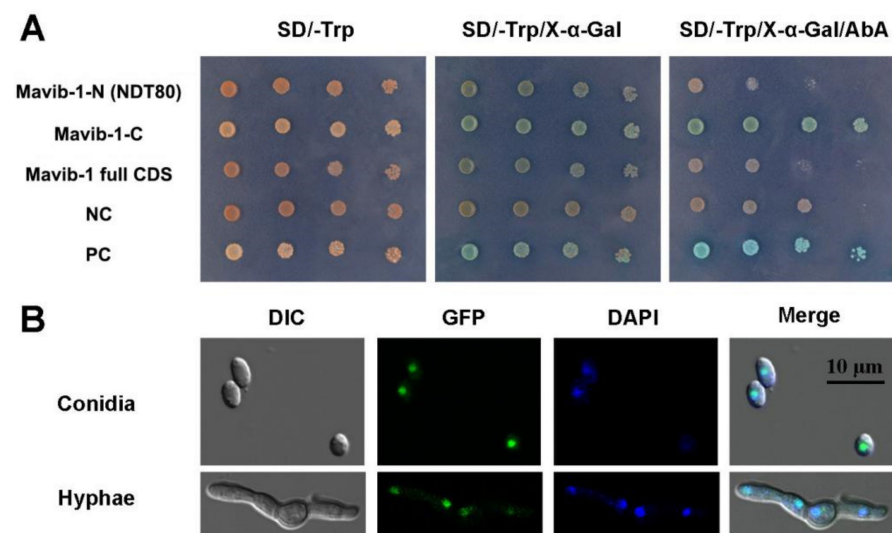


**Figure 1.** Transcriptional-activation assays and subcellular localization of *Mavib-1*. (A) Transcriptional activation assays in yeast. *Mavib-1-N* (containing NDT80 domain), *Mavib-1-C* or *Mavib-1* full CDS were fused to the GAL4 DNA-binding domain and expressed in yeast strain Y2H Gold. Strain containing only GAL4 DNA-binding domain was as negative control (NC), containing the GAL4 DNA-binding and activation domains were as positive controls (PC). All the yeast strains were cultured on SD-Trp plates, SD-Trp plates containing 0.5 mM X- $\alpha$ -gal and SD-Trp plates containing 0.5 mM X- $\alpha$ -gal and 200 ng/mL

AbA (Aureobasidin A) at 30 °C for 3 days. (B) Subcellular localization of Mavib-1. The expression of *Mavib-1* and *EGFP* fusion protein was driven by strong promoter *PgpdM*. The conidia and mycelia of OE strain were stained with DAPI (4',6-diamidino-2-phenylindole, C0065, Solarbio, China), a fluorescent dye that can bind strongly to DNA, and observed under a confocal microscope (TCS SP8, Leica, Germany).

### 3.3. *Mavib-1* Affected Stress Tolerances of *M. acridum*

Stress tolerances are very important characteristics for fungal potential against insect pests. Compared to the WT, the  $\Delta$ *Mavib-1* mutant showed a significant change in conidial sensitivity to UV radiation and heat stress (Figure 2). After UV-B irradiation, conidial germination and mean  $IT_{50}$  values of  $\Delta$ *Mavib-1* mutant were significantly decreased compared to WT, while OE strain did not show significant difference compared to WT (Figure 2A,B). After heat treatment, both  $\Delta$ *Mavib-1* and OE strains presented a significant decrease in conidial germination and mean  $IT_{50}$  values compared to WT, but  $\Delta$ *Mavib-1* showed a sharply decreased in heat treatment (Figure 2C,D). CP strain showed a partial recovery in UV-B and heat stress tolerance compared to WT and  $\Delta$ *Mavib-1* mutant.

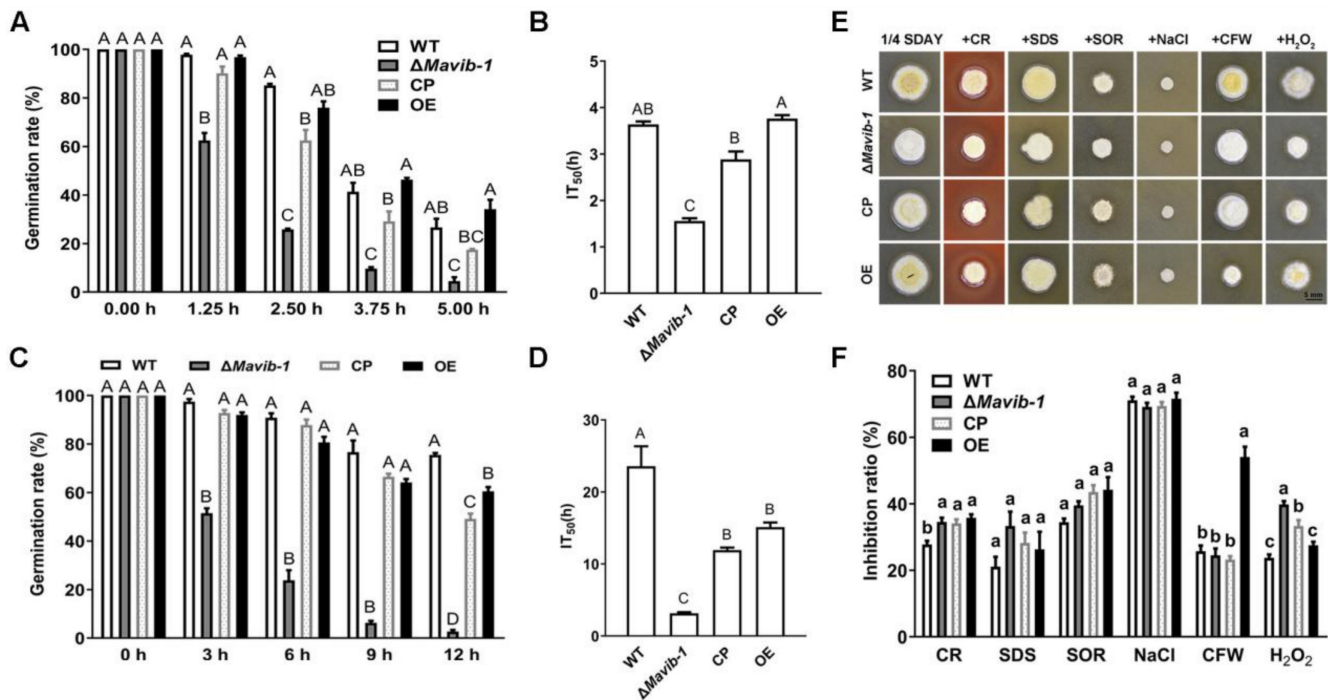


**Figure 2.** Stress tolerances of conidia from WT,  $\Delta$ *Mavib-1*, CP and OE strains. (A) Germination rate of each strain on 1/4 SDAY media at 28 °C for 20 h after UV-B stress treatment at 0, 1.25, 2.5, 3.75, 5.0 h. (B) The half inactivity time ( $IT_{50}$ ) of each strain with UV-B treatment. (C) Germination rates on 1/4 SDAY at 28 °C for 20 h after 46 °C heat stress treatment at 0, 3, 6, 9, 12 h. (D) The  $IT_{50}$  of WT,  $\Delta$ *Mavib-1*, CP and OE strains under 46 °C heat treatment. (E) The fungal colony on 1/4 SDAY medium and 1/4 SDAY with cell wall disruptors (500  $\mu$ g/mL CR, 50  $\mu$ g/mL CFW), cell wall stressor (0.01% SDS), hyperosmotic stressors (1 mol/L SOR or 1 mol/L NaCl), oxidative stress (6 mmol/L  $H_2O_2$ ), respectively. (F) Inhibition rate of colony growth. All experiments were repeated three times for statistical analysis. Different capital letters represented significant difference at  $p < 0.01$ ; different lower-case letters represented significant difference at  $p < 0.05$ .

$\Delta$ *Mavib-1* and OE did not show significant difference in tolerance to SDS, SOR and NaCl compared to WT. The OE strain had more sensitivity to CR and CFW, while  $\Delta$ *Mavib-1* had weaker tolerance to CR and  $H_2O_2$  (Figure 2E,F), indicating a destroyed cell wall integrity in  $\Delta$ *Mavib-1* and OE strains.

### 3.4. Disruption of *Mavib-1* Affected Conidial Germination, Conidial Cell Wall Surface Ultrastructure, and Conidial Hydrophobicity

Germination rates of conidia of WT,  $\Delta Mavib-1$ , CP and OE strains were determined on 1/4 SDAY at different culture intervals. Results showed that  $GT_{50}$  of  $\Delta Mavib-1$  and OE strains were significantly prolonged than that of WT (Figure 3A). The *Mavib-1* gene affected the resistance to cell-wall-disrupting agent CFW (Figure 2E,F); we speculated that *Mavib-1* might affect the conidial cell wall structure. SEM analysis showed that the conidial surface of WT and OE strains had a rough cell wall surface, while the  $\Delta Mavib-1$  strain had a smoother cell wall surface compared with WT (Figure 3B).

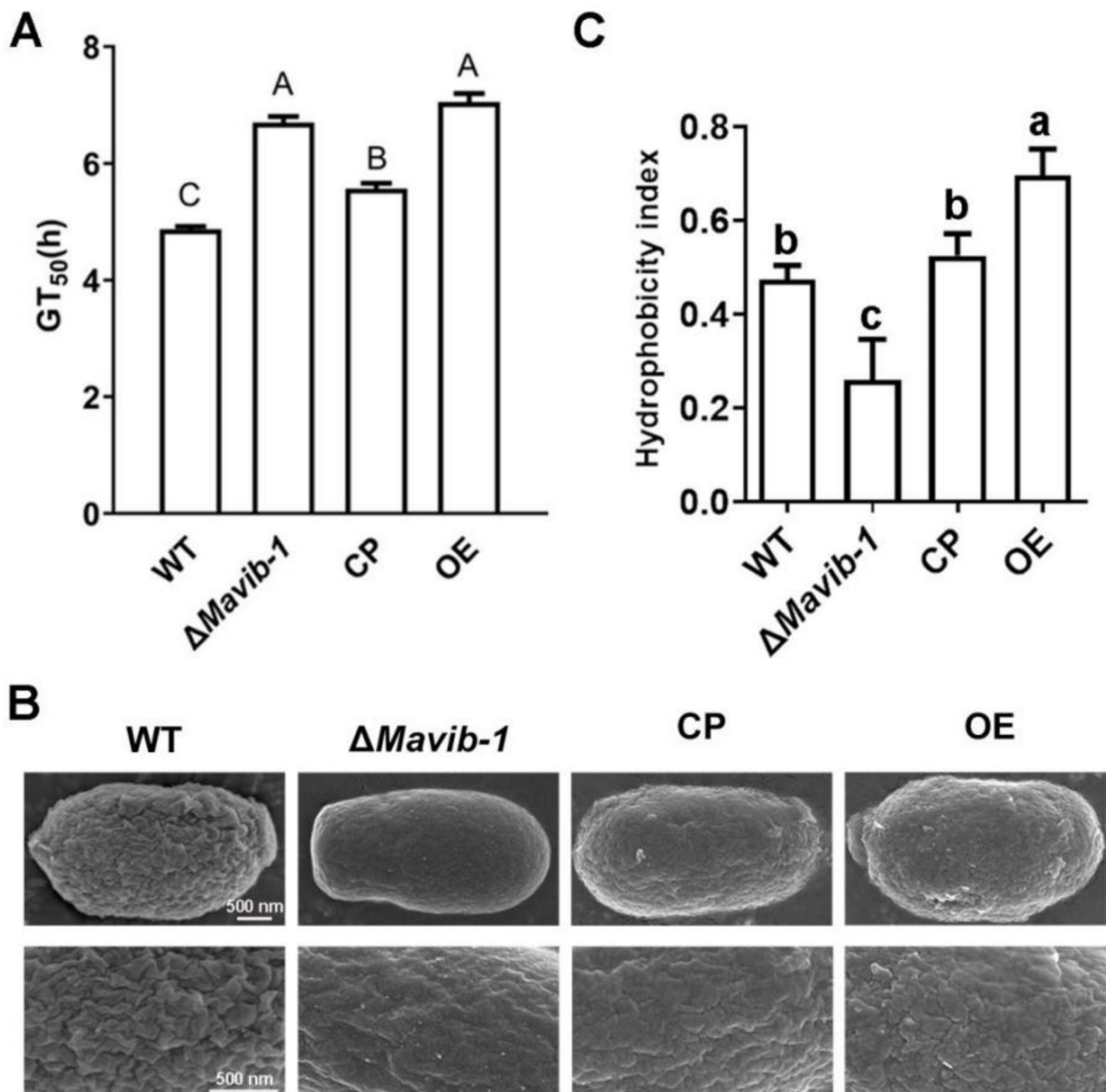


**Figure 3.** Conidial germination, conidial surface morphology and hydrophobicity determination. (A) The 50% germination times ( $GT_{50}$ ) of WT,  $\Delta Mavib-1$ , CP and OE strains. (B) The conidial surface morphology by SEM. (C) Conidial hydrophobicity index. The trial was repeated three times. Different capital letters represented significant difference at  $p < 0.01$  and different lower-case letters indicate significant difference,  $p < 0.05$ .

The structure of the fungal cell wall surface is closely related to the conidial characteristics. The rodlets on the conidial surface are arranged according to certain rules by fungal hydrophobins [31]. Hydrophobicity assay showed that the conidial hydrophobic index was significantly decreased in  $\Delta Mavib-1$  and significantly increased in OE strain compared to WT (Figure 3C). These results indicated that deletion of *Mavib-1* affected conidial germination, conidial cell wall surface ultrastructure and conidial hydrophobicity in *M. acridum*.

### 3.5. Disruption of *Mavib-1* Affected Growth and Conidiation of *M. acridum* on Different Carbon or Nitrogen Source Media

*Mavib-1* has a nutrient sensing-related NDT80\_PhoG domain, and the growth, conidiation and conidial yield of WT,  $\Delta Mavib-1$ , CP and OE strains on media with different carbon and nitrogen sources were determined. On the nutrient-rich medium 1/4 SDAY,  $\Delta Mavib-1$  and OE strains had similar colony color and size compared to WT. On nutrient-limited media, in which glucose, sucrose or glycerol was used as the main carbon source, respectively, or no extra carbon source was added,  $\Delta Mavib-1$  colony had a much lighter color and significantly smaller size than WT, while the OE strain had a similar colony phenotype as WT. Conidial production analysis showed that deletion of *Mavib-1* resulted in decreased conidial yield of *M. acridum* regardless of rich nutrient or starvation (Figure 4C). These results indicated that *Mavib-1* gene is necessary for colony growth and the conidial melanin formation under nutrient deficiency in *M. acridum*. Microscopic observation showed that the  $\Delta Mavib-1$  strain performed normal conidiation similar to WT and OE at the early growth time on 1/4 SDAY (12 h and 24 h). However,  $\Delta Mavib-1$  strain produced more conidia than WT and OE at 36 h. Conidiation was also analyzed on SYA, a microcycle conidiation medium for *M. acridum* [4]. It clearly showed that WT and  $\Delta Mavib-1$  conducted MC, while the OE strain changed to typical hyphal growth and conducted normal conidiation. On other media without a carbon source, or with glucose and glycerol as carbon source,  $\Delta Mavib-1$  exhibited normal conidiation slightly earlier than WT, while the OE strain did not show conidiogenous structure until 36 h (Figure 4D).

Similar to the role in carbon source utilization, *Mavib-1* also contributed to the utilization of different nitrogen sources, including dominant (glutamine) and non-dominant (urea and  $\text{NaNO}_3$ ) nitrogen sources (Figure 5A).  $\Delta Mavib-1$  colonies were whitish in color on SYA medium with different nitrogen sources (Figure 5A) and had significantly smaller size than WT and CP, when urea or  $\text{NaNO}_3$  was used as the main nitrogen source or no extra nitrogen source (SYA-N) was included, while the OE strain had an obviously larger colony on these media (Figure 5A,B). These results indicated that *Mavib-1* positively regulated fungal growth by affecting utilization of nitrogen sources. Conidial yield analysis showed that  $\Delta Mavib-1$  had significantly decreased conidia production compared to WT when urea or  $\text{NaNO}_3$  was used as main nitrogen source, while overexpression of *Mavib-1* did not significantly affect conidial yield in *M. acridum* (Figure 5C). Microscopic observation showed that, similar as the results on the media with different carbon sources,  $\Delta Mavib-1$  strain performed MC on SYA-N and SYA medium slightly earlier compared to WT. WT strain performed hyphal growth at 20 h, while  $\Delta Mavib-1$  strain had already produced a mass of conidia at that time. Conidiation of OE strain was drastically delayed compared with WT on different nitrogen source media, and no conidia was formed until 36 h on the SYA-N and SYA-Urea media (Figure 5D). These results indicated that *Mavib-1* positively regulated fungal growth and negatively regulated conidiation of *M. acridum* by affecting utilization of different carbon or nitrogen sources especially when nutrient was insufficient. However, *Mavib-1* contributed to total conidial yield in *M. acridum* under both nutrient-rich and nutrient-limited conditions.



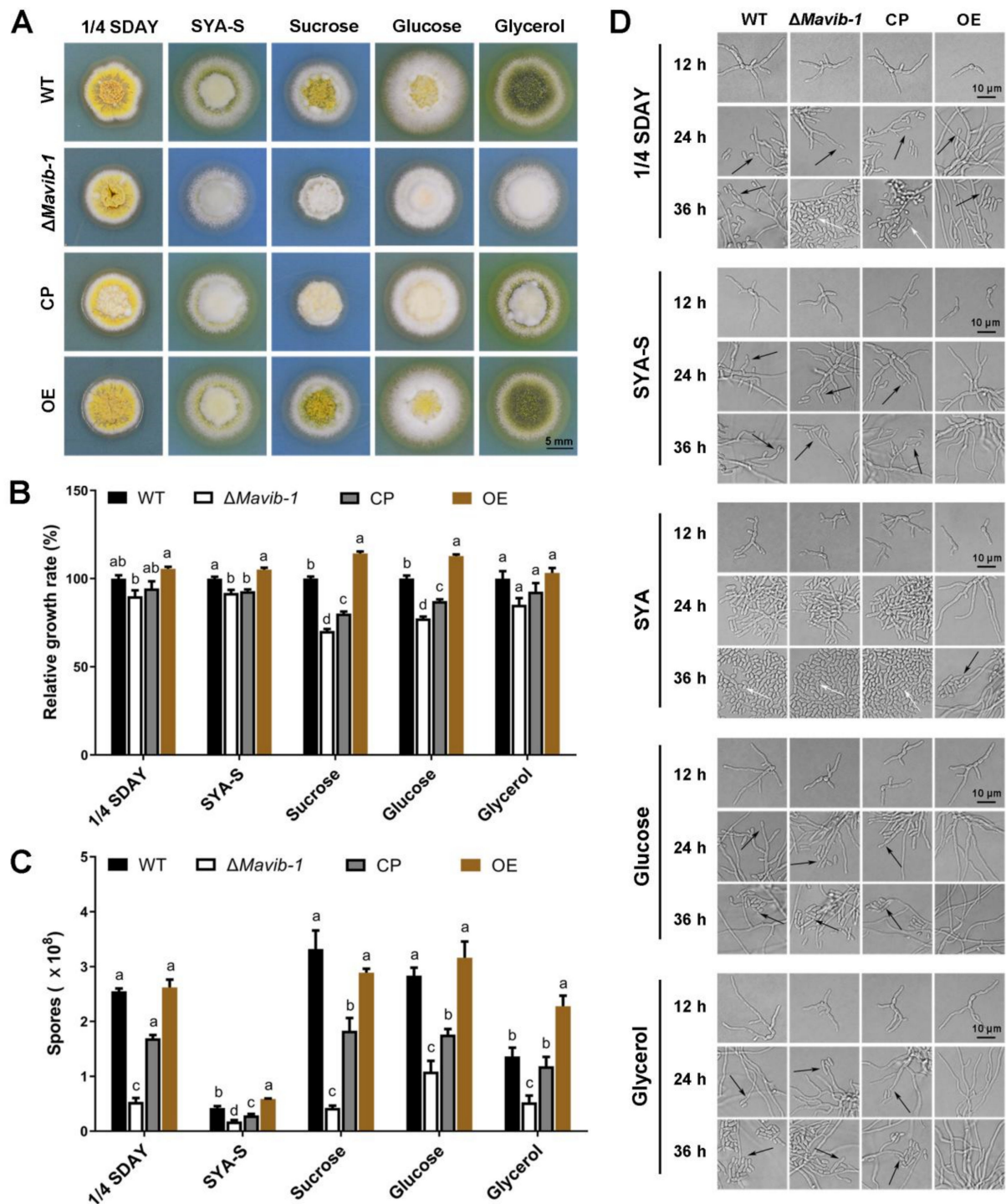


**Figure 4.** Colony growth and conidiation of fungal strains on media containing different carbon sources. (A) Colony morphology of WT,  $\Delta Mavib-1$ , CP and OE strains. Fungal strains were cultured on the nutrient-rich medium 1/4 SDAY, and nutrient-limited medium SYA with easy-to-use or difficult-to-use carbon sources (3% w/v; easy to use: glucose; middle: sucrose, difficult to use: glycerol) for 5 d. Colony relative growth rate (B) and conidial yield (C) of WT,  $\Delta Mavib-1$ , CP and OE strains cultured on 1/4 SDAY or SYA with different carbon sources for 5 d. The trial was repeated three times. Error bars are standard deviations of three replicates. Different lower-case letters indicate significant difference at  $p < 0.05$ . (D) Conidiation of WT,  $\Delta Mavib-1$ , CP and OE strains on different media. The black arrows indicate normal conidiation, and the white arrows indicate microcycle conidiation.

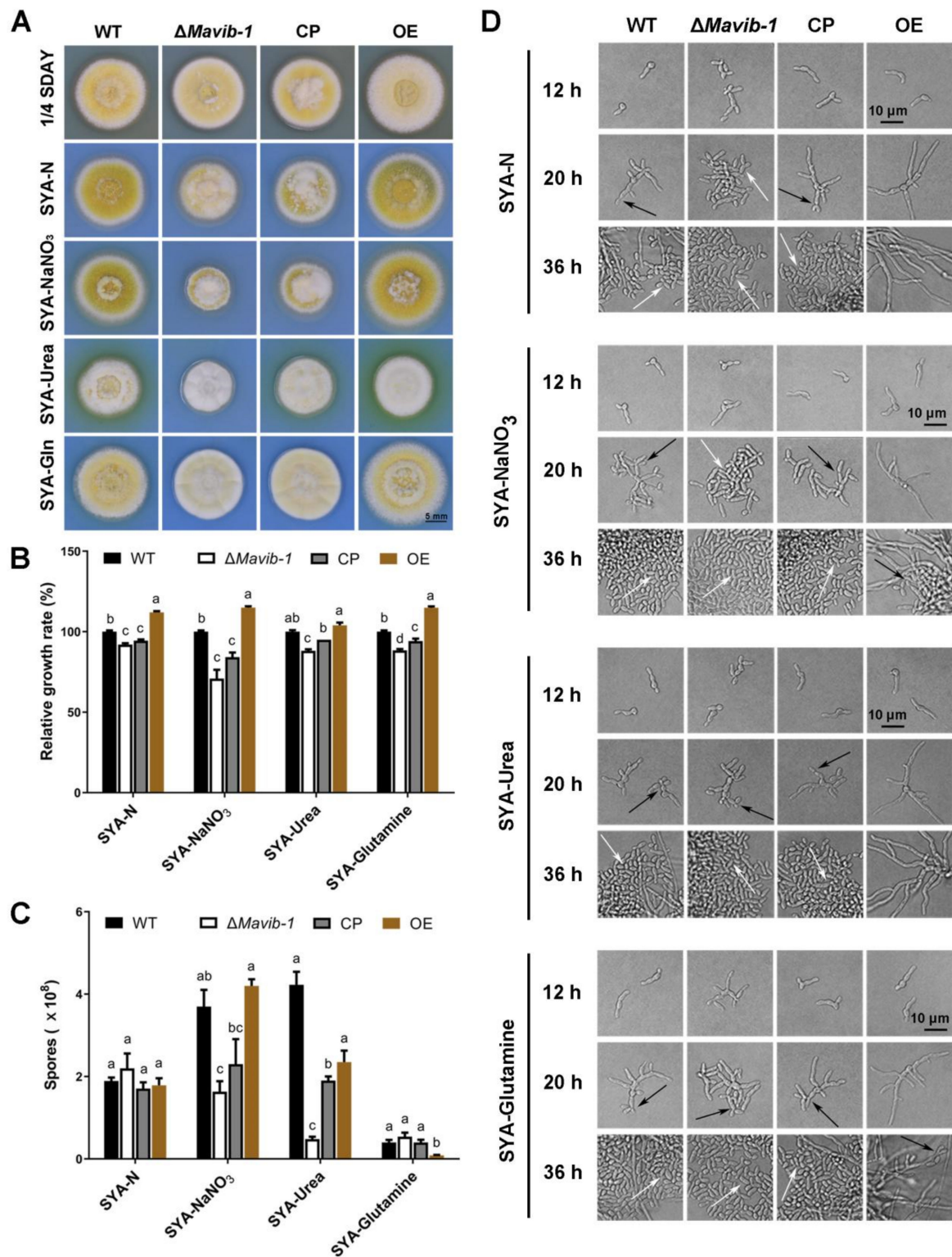


**Figure 5.** Colony growth and conidiation of  $\Delta Mavib-1$ , CP and OE strains on media with different nitrogen sources. Colony morphology (A) and colony relative growth rate (B) of  $\Delta Mavib-1$ , CP and OE strains on the media 1/4 SDAY, and SYA with different nitrogen sources. (C) Conidial yield of fungal strains cultured on different media for 15 d. Media contained 0.3% nitrogen source: SYA-N (SYA without NaNO<sub>3</sub>), urea (difficult to use), NaNO<sub>3</sub> (middle), Gln (easy to use). Each trial was repeated three times for statistical analysis. Different lower-case letters mean significant difference at  $p < 0.05$ . (D) Conidiation of  $\Delta Mavib-1$ , CP and OE strains on different media. The black arrows indicate NC, and the white arrows indicate MC.

### 3.6. *Mavib-1* Affected Expression of CAZyme Genes of *M. acridum*

To elucidate the mechanism by which *Mavib-1* affects the conidiation of *M. acridum* in response to different carbon and nitrogen sources, RNA-seq was performed for WT,  $\Delta$ *Mavib-1* and OE strains cultured on SYA medium for 20 h (Accession No. PRJNA73660). The RNA-seq data were verified by RT-qPCR, and the difference fold changes obtained by the two methods were extremely significantly correlated ( $R = 0.890$  and  $p < 0.01$  in  $\Delta$ *Mavib-1*,  $R = 0.960$  and  $p < 0.01$  in OE), indicating that the RNA-seq data were reliable (Table S2). Primer sequences used for verification are listed in Table S1.

Statistical analysis was performed on the RNA-seq data of three groups. The correlation heat map showed that the correlation between the three replicates in each group was high, and the correlation between groups was small, indicating a good repeatability of sequence data (Figure S3A). Principal component analysis (PCA) showed that the three replicates in each group could be clustered together, again indicating that the data were reproducible (Figure S3B). The RNA-seq data were screened after quality control and qPCR validation and genes with  $|\log_2FC| \geq 1$ ,  $Qvalue \leq 0.01$  and  $FPKM \geq 5$  were counted as DEGs (Tables S3 and S4). RNA-seq showed that there were a total of 291 DEGs (79 up-regulated, 212 down-regulated) in the  $\Delta$ *Mavib-1* strain, and a total of 486 DEGs (318 up-regulated and 168 down-regulated) in the OE strain (Figure 6A) compared to WT. The Venn diagram showed that there were 101 shared DEGs between  $\Delta$ *Mavib-1* and OE (66 DEGs both down-regulated, 13 DEGs both up-regulated, and 18 DEGs down-regulated in  $\Delta$ *Mavib-1* and up-regulated in OE, 4 DEGs up-regulated in  $\Delta$ *Mavib-1* and down-regulated in OE) (Figure 6B). The detailed information of 22 DEGs (18 downregulated and 4 upregulated in  $\Delta$ *Mavib-1*), with opposite changing trend of transcription in  $\Delta$ *Mavib-1* and OE, is listed in Table S5. To intuitively reflect these DEGs with the opposite changing trend, a cluster heat map of 22 DEGs was constructed (Figure 6C,D).

GO classification (Figure S4), KEGG enrichment (Figure S5) and carbohydrate activity enzymes (CAZymes) annotation analysis were performed for DEGs. The up-regulated genes in  $\Delta$ *Mavib-1* strain were mainly enriched in RNA polymerase, nitrogen metabolism and atrazine degradation, etc., and the down-regulated genes were mainly enriched in neuroactive ligand–receptor interaction, protein digestion and absorption, pancreatic secretion, influenza A and glycerolipid metabolism, etc. (Figure S5A,B). The upregulated genes in the OE strain were mainly enriched in microbial metabolism in diverse environment, metabolic pathways, and beta-alanine metabolism, etc. The downregulated genes were mainly enriched in amino sugar and nucleotide sugar metabolism, phenylpropanoid biosynthesis, neuroactive ligand–receptor interaction, protein digestion and absorption and metabolic pathways, etc. (Figure S5C,D). These results indicated that *Mavib-1* affected the carbon and nitrogen source metabolic pathways of *M. acridum*. Aligning the DEGs with the CAZy database [32] revealed that many DEGs belong to CAZymes (9 of the 291 DEGs in the  $\Delta$ *Mavib-1* strain listed in Table S6, and 41 of the 486 DEGs in the OE strain listed in Table S7). Cluster heatmap of DEGs belonging to CAZymes showed that the expression of CAZyme genes in  $\Delta$ *Mavib-1* and OE strains have changed (Figure 6E,F), indicating that *Mavib-1* played an important role in regulation of the expression of CAZyme genes in *M. acridum*. At the same time, 21 nitrogen source metabolism-related genes (listed in Table S8) were also found in DEGs. The transcription changes of these nitrogen metabolism and conidiation related genes in  $\Delta$ *Mavib-1* and OE strains may provide explanations for the effects of *Mavib-1* on nitrogen metabolism and conidiation in *M. acridum*.



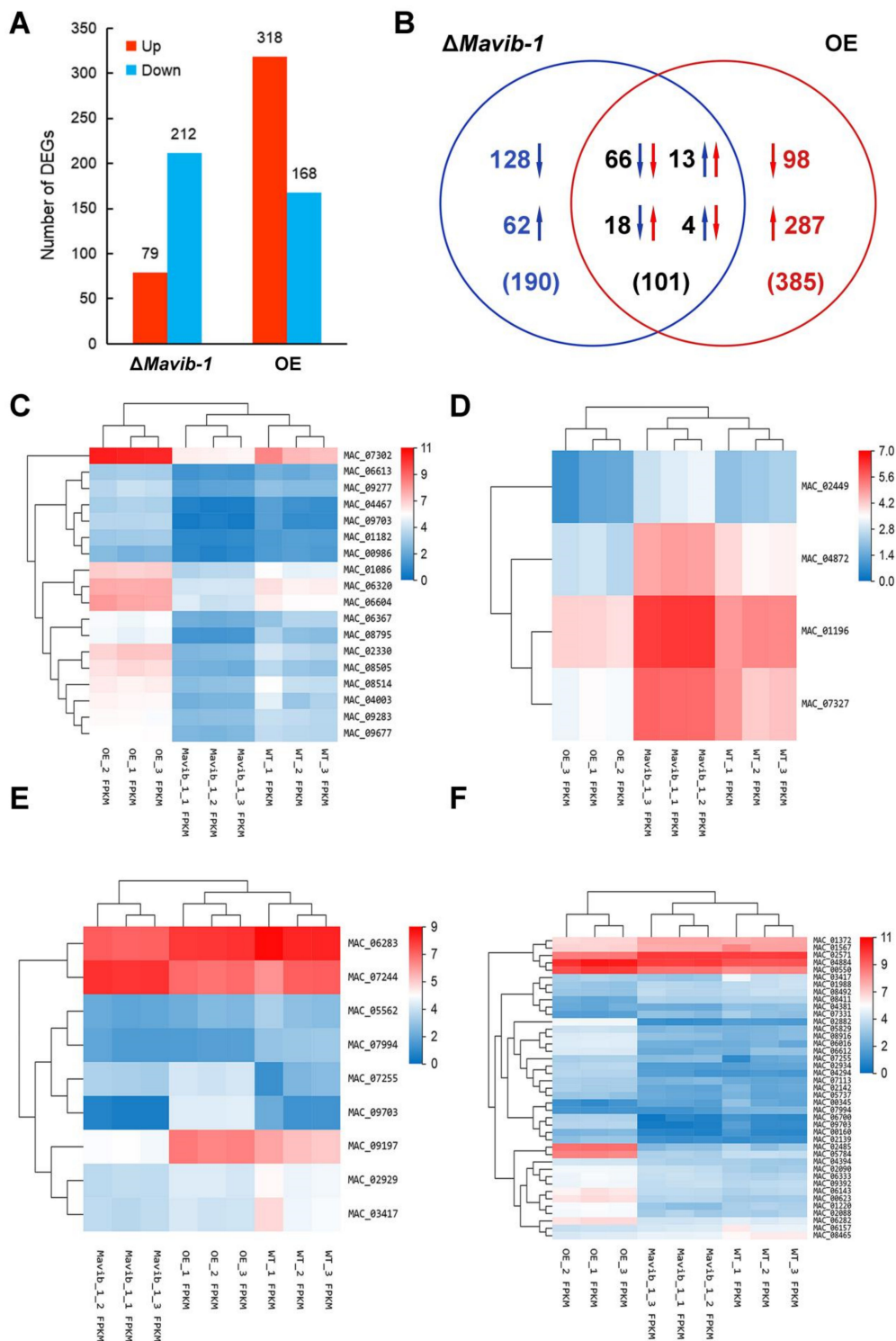


**Figure 6.** DEGs analysis. (A) Statistical histogram of the number of DEGs. (B) Venn diagram of DEGs. (C) Heat map of 18 DEGs downregulated in  $\Delta Mavib-1$  and upregulated in OE. The 18 DEGs consistent with the change trend of *Mavib-1* were analyzed by cluster analysis of expression patterns. The distance calculation method was used: the spearman correlation coefficient between samples, the Pearson correlation coefficient between genes. (D) Cluster heat map of the expression levels of the 4 genes upregulated in  $\Delta Mavib-1$  and downregulated in OE. (E) Heat map of the expression of DEGs in  $\Delta Mavib-1$  annotated as CAZyme genes. (F) Heat map of the expression of DEGs in OE annotated as CAZyme genes. The up and down arrows represent upregulated or downregulated genes, respectively. Numbers in blue represent  $\Delta Mavib-1$  and red represent OE. The red color denotes the upregulated DEGs, and the blue color denotes downregulated DEGs. The  $\log_2$  (expression value + 1) of the sample were shown in the horizontal axis, and DEGs are shown at the right-hand vertical side.



#### 4. Discussion

The growth and development of filamentous fungi require suitable conditions such as temperature, humidity, pH, and nutrients. Filamentous fungi can sense the nutrient conditions in the environment and regulate their development. In this study, we demonstrated the role of *Vib-1* in NC and MC by affecting the nutrition utilization in entomopathogenic fungus *M. acridum*.

*Mavib-1* shares the NDT80\_PhoG domain with Ndt80 of *S. cerevisiae* [33], *Vib-1*, Fsd-1 and NCU04729 of *N. crassa* [34,35], and XprG and NdtA of *A. nidulans* [36–38]. *Mavib-1* was localized at nuclear in both conidia and hyphae, while *Vib-1*-GFP was found in nuclear in hyphae and cytoplasmically localized in conidiophores and immature conidia in *N. crassa* [21]. This might cause some divergent roles of *Vib-1* in different fungi. Proteins containing NDT80\_PhoG domains had been reported in model fungi yeast and *N. crassa*. In *S. cerevisiae*, Ndt80 is a meiosis-specific transcription factor that regulates the expression of metaphase genes and also regulated by the pachytene checkpoint [39–41]. In filamentous fungi, sporogenesis is a procedure of producing a new cell through cell division by mitosis, which *Vib-1* might be involved in the regulation of conidiation. Consistent with our result, *Vib-1* was involved in the regulation of conidiation in *N. crassa* [21].

Our findings indicate that *Mavib-1* positively regulates fungal growth, and negatively regulates conidiation especially under nutrient deficient conditions. Consistent with the decreased hyphal extension in *Vib-1* disruption mutant in *N. crassa* [21],  $\Delta$ *Mavib-1* had shortened hyphae when growing on nutrient-rich medium. However, conidiation was decreased in  $\Delta$ *Mavib-1* and showed no changes when *Mavib-1* was upregulated, in contrast with no changes in *Vib-1* mutant and decreased conidiation in *Vib-1* overexpression strain in *N. crassa* [21], indicating a divergent role of *Vib-1* in different fungi. When under carbon-limited conditions, deletion of *N. crassa Vib-1* causes a growth defect on cellulose biomass [23]. Some other Ndt80-containing proteins were reported to contribute to growth and nutrient utilization. Ndt80 transcription factor RON1 is essential for hyphal growth and N-acetylglucosamine (GlcNAc) metabolism in *Cryptococcus neoformans* [42]. In *A. nidulans*, the Ndt80-like protein XprG positively regulates the expression of extracellular proteases, mycotoxins and penicillins in response to carbon starvation [37]. In *M. acridum*, disruption of the *Vib-1* led to a more serious defect in growth and conidiation initiation under carbon and nitrogen limited condition, but OE strain displayed a contrast phenotype with  $\Delta$ *Mavib-1*, demonstrating more important roles of *Mavib-1* in both carbon and nitrogen utilization under nutrient limitation. Therefore, the explanation for the conidiation pattern change of *Mavib-1* mutants was as follows. When *Mavib-1* was impaired, *M. acridum* could not obtain enough nutrients to support hyphal growth and then the conidiation was induced, while hyphal growth was retained and strengthened owing to an improvement of nutrient utilization during overexpression of *Mavib-1*.

Consistent with the inhibited hyphal growth in  $\Delta$ *Mavib-1* and promoted growth in OE strain on plate, RNA-Seq analysis revealed that DEGs of  $\Delta$ *Mavib-1* and OE strains included many CAZyme members, which can degrade, modify or create glycosidic bonds. In  $\Delta$ *Mavib-1*, the DEGs related to CAZyme were mostly downregulated (seven downregulated in nine DEGs) compared to upregulation of most CAZyme DEGs (27 upregulated in 41 DEGs) in OE strain. This indicated a more active carbon metabolism when *Mavib-1* was overexpressed. Similar in *N. crassa*, *Vib-1* can repress glucose signaling and CCR [23], and cellulose digestion-related genes were increased and glucose metabolism related CAZyme were repressed under carbon starvation [22,23] in *Vib-1* disruption mutant.

In *Aspergillus niger*, nutrient limitation, such as severe carbon limitation, led to a zero growth rate and induction of conidiation [43,44]. *M. acridum* show similar growth phenotype on minimal medium (Figure S6A), on which all WT and mutant strains conducted MC and no hyphal growth was observed under microscope (Figure S6B). This made it impossible to analyze the shift between hyphal growth and conidiation. On minimal medium, OE strain had a larger colony size and a better growth than  $\Delta$ *Mavib-1*, which was consistent with the result on nutrient-limited medium SYA (Figure S6A). Therefore, we preferred

analysis of hyphal growth and conidiation on nutrient-limited media SYA, on which *M. acridum* might change to normal conidiation when conidiation was in dysregulation.

The fungal cell wall acts as an environmental barrier to the host immune system and plays a crucial role in the pathogenic process and stress tolerance of entomopathogenic fungi [45]. Elements involved in pathways of cell wall integrity would affect the fungal virulence and stress tolerance to heat, UV irradiation or chemical stressors [46–48]. In *M. acridum*, *Vib-1* disruption or overexpression affected many genes related to CAZyme, which would also affect the cell wall synthesis. The conidial pigment formation-related gene laccase, also a virulence factor [49], was downregulated in  $\Delta Mavib-1$  and upregulated in OE strain (Table S5), which was consistent with the light color of colony and decreased pathogenicity in  $\Delta Mavib-1$ . Agreed with decreased UV tolerance, riboflavine-aldehyde-forming enzyme gene (MAC\_01768), contributed to UV tolerance and virulence in *Metarhizium* [50], was significantly downregulated in  $\Delta Mavib-1$ . SEM showed that  $\Delta Mavib-1$  had abnormal conidial surface morphology compared to WT and OE. These changes in gene transcription or cell wall structure might lead to changes tolerance to environmental stresses and virulence.  $\Delta Mavib-1$  did not show opposite transcription changes with *Mavib-1*-OE strain in all the tested phenotype, such as decreased virulence, decreased UV and heat tolerance in  $\Delta Mavib-1$ , while there were no changes for these phenotypes in OE. This may be due to the complexity of biological regulation. After a gene is knocked out or overexpressed, it may lead to expression changes of other related genes to make up for the defects, and finally result in an atypical phenotype. Previous reports showed that the damage of conidial cell wall surface results in reduced pathogenicity, but enhanced thermotolerance in *B. bassiana* [31]. Moreover, conidial characteristics are closely related to the adherence and invasion ability of entomopathogenic fungi [29,51]. The changes in conidial characteristics in  $\Delta Mavib-1$  would possibly affect the fungal pathogenicity. Some pathogenicity-related genes were also affected by *Mavib-1*. For example, citrinin biosynthesis transcriptional activator CtnR [52] and polyketide synthase protein (MAC\_01101) [53], were differentially expressed in  $\Delta Mavib-1$  or OE strains (Tables S3 and S4). These results suggested that *Vib-1* might contribute to virulence in *M. acridum*.

## 5. Conclusions

In summary, our study indicated that the transcription factor *Mavib-1* positively regulated fungal growth and negatively regulated conidiation by affecting utilization of carbon and nitrogen sources in *M. acridum*. Owing to the contribution in the regulation of nutrient utilization, *Mavib-1* contributed to the conidiation pattern shift from microcycle conidiation to normal conidiation under nutrient deficiency. Moreover, *Mavib-1* is important for stress tolerance in *M. acridum*. Further analysis of the divergent upstream and downstream targets of *Mavib-1* in regulating fungal growth, conidiation, stress tolerance and virulence will help explore the underlying regulative mechanisms of *Vib-1* in response to nutrient and other environmental stimuli.

**Supplementary Materials:** The following supporting information can be downloaded at: <https://www.mdpi.com/article/10.3390/jof8060594/s1>, Figure S1: Sequence analysis of *Mavib-1*. Figure S2: Construction of *Mavib-1* disruption ( $\Delta Mavib-1$ ), complementation (CP) and overexpression (OE) strains of the *Mavib-1* gene in *M. acridum*. Figure S3: RNA-seq data quality control analysis. Figure S4: GO classification of DEGs. Figure S5: DEGs KEGG pathway enrichment analysis. Figure S6: Colony growth and conidiation of WT,  $\Delta Mavib-1$ , CP and OE strains on minimal medium (CZA). Table S1: Primers used in construction of *Mavib-1* deletion mutant, complemented strain and overexpression. Table S2: Verification of DEGs results by RT-qPCR analysis. Table S3: DEGs of  $\Delta Mavib-1$  compared to WT cultured on SYA medium for 20 h. Table S4: DEGs of *Mavib-1* OE compared to WT cultured on SYA medium for 20 h. Table S5: DEGs with opposite changing trends of transcription in  $\Delta Mavib-1$  and OE. Table S6: CAZyme in DEGs of  $\Delta mavib-1$ . Table S7: CAZyme in DEGs of OE. Table S8: DEGs related to nitrogen metabolism.

**Author Contributions:** Conceptualization, Y.C.; Methodology, X.S.; Validation, X.S. and H.L.; Investigation, X.S.; Resources, Y.C. and Y.X.; Writing—Original Draft Preparation, X.S.; Writing—

Review and Editing, Y.C. and Y.X.; Visualization, X.S.; Supervision, Y.C. and Y.X.; Project Administration, Y.C.; Funding Acquisition, Y.C. All authors have read and agreed to the published version of the manuscript.

**Funding:** This study was supported by Natural Science Foundation of China (No. 31772222) and Natural Science Foundation Project of CQ CSTC (cstc2021jcyj-msxmX0261).

**Institutional Review Board Statement:** Not applicable.

**Informed Consent Statement:** Not applicable.

**Data Availability Statement:** The data presented in this study are available in this article and its Supplementary Materials.

**Conflicts of Interest:** The authors declare no conflict of interest.

## References

- Pendland, J.C.; Hung, S.Y.; Boucias, D.G. Evasion of host defense by in vivo-produced protoplast-like cells of the insect mycopathogen *Beauveria bassiana*. *J. Bacteriol.* **1993**, *175*, 5962–5969. [\[CrossRef\]](#)
- Khurana, N.; Saxena, R.K.; Gupta, R.; Kuhad, R.C. Light-independent conidiation in *Trichoderma* spp.: A novel approach to microcycle conidiation. *World J. Microbiol. Biotechnol.* **1993**, *9*, 353–356. [\[CrossRef\]](#) [\[PubMed\]](#)
- Clarkson, J.M.; Charnley, A.K. New insights into the mechanisms of fungal pathogenesis in insects. *Trends Microbiol.* **1996**, *4*, 197–203. [\[CrossRef\]](#)
- Zhang, S.Z.; Peng, G.X.; Xia, Y.X. Microcycle conidiation and the conidial properties in the entomopathogenic fungus *Metarhizium acridum* on agar medium. *Biocontrol Sci. Technol.* **2010**, *20*, 809–819. [\[CrossRef\]](#)
- De Faria, M.R.; Wraight, S.P. Mycoinsecticides and mycoacaricides: A comprehensive list with worldwide coverage and international classification of formulation types. *Biol. Control* **2007**, *43*, 237–256. [\[CrossRef\]](#)
- St. Leger, R.J.; Wang, C. Genetic engineering of fungal biocontrol agents to achieve greater efficacy against insect pests. *Appl. Microbiol. Biot.* **2010**, *85*, 901–907. [\[CrossRef\]](#)
- Ortiz-Urquiza, A.; Luo, Z.; Keyhani, N.O. Improving mycoinsecticides for insect biological control. *Appl. Microbiol. Biot.* **2015**, *99*, 1057–1068. [\[CrossRef\]](#)
- Peng, G.; Xia, Y. The mechanism of the mycoinsecticide diluent on the efficacy of the oil ormlulation of insecticidal fungus. *Biocontrol* **2011**, *56*, 893–902. [\[CrossRef\]](#)
- Wang, C.S.; Wang, S.B. Insect pathogenic fungi: Genomics, molecular interactions, and genetic improvements. *Annu. Rev. Entomol.* **2017**, *62*, 73–90. [\[CrossRef\]](#)
- Hanlin, R. Microcycle conidiation-A review. *Mycoscience* **1994**, *35*, 113–123. [\[CrossRef\]](#)
- Anderson, J.G.; Smith, J.E. The production of conidiophores and conidia by newly germinated conidia of *Aspergillus niger* (microcycle conidiation). *J. Gen. Microbiol.* **1971**, *69*, 185–197. [\[CrossRef\]](#) [\[PubMed\]](#)
- Bosch, A.; Yantorno, O. Microcycle conidiation in the entomopathogenic fungus *Beauveria bassiana* bals. (vuill.). *Process Biochem.* **1999**, *34*, 707–716. [\[CrossRef\]](#)
- Park, H.S.; Yu, J.H. Genetic control of asexual sporulation in filamentous fungi. *Curr. Opin. Microbiol.* **2012**, *15*, 669–677. [\[CrossRef\]](#) [\[PubMed\]](#)
- Zhang, S.Z.; Xia, Y.X. Identification of genes preferentially expressed during microcycle conidiation of *Metarhizium anisopliae* using suppression subtractive hybridization. *FEMS Microbiol. Lett.* **2008**, *286*, 71–77. [\[CrossRef\]](#)
- Sekiguchi, J.; Gaucher, G.M.; Costerton, J.W. Microcycle conidiation in *Penicillium urticae*: An ultrastructural investigation of conidiogenesis. *Can. J. Microbiol.* **1975**, *21*, 2069–2083. [\[CrossRef\]](#)
- Gestel, J.F.E.V. Microcycle conidiation in *Penicillium italicum*. *Exp. Mycol.* **1983**, *7*, 287–291. [\[CrossRef\]](#)
- Vézina, C.; Singh, K.; Sehgal, S.N. Sporulation of filamentous fungi in submerged culture. *Mycologia* **1965**, *57*, 722–736. [\[CrossRef\]](#)
- Saxena, R.K.; Khurana, N.; Kuhad, R.C.; Gupta, R. D-glucose soluble starch, a novel medium for inducing microcyclic conidiation in *Aspergillus*. *Mycol. Res.* **1992**, *96*, 490–494. [\[CrossRef\]](#)
- Ahearn, D.G.; Price, D.; Simmons, R.B.; Mavo, A.; Zhang, S.T.; Crow, S.A. Microcycle conidiation and medusa head conidiophores of *Aspergilli* on indoor construction materials and air filters from hospitals. *Mycologia* **2007**, *99*, 1–6. [\[CrossRef\]](#)
- Wang, Z.L.; Jin, K.; Xia, Y.X. Transcriptional analysis of the conidiation pattern shift of the entomopathogenic fungus *Metarhizium acridum* in response to different nutrients. *BMC Genom.* **2016**, *17*, 586. [\[CrossRef\]](#)
- Dementhon, K.; Iyer, G.; Glass, N.L. VIB-1 is required for expression of genes necessary for programmed cell death in *Neurospora crassa*. *Eukaryot. Cell* **2006**, *5*, 2161–2173. [\[CrossRef\]](#) [\[PubMed\]](#)
- Wu, V.W.; Thieme, N.; Huberman, L.B.; Dietschmann, A.; Kowbel, D.J.; Lee, J.; Calhoun, S.; Singan, V.R.; Lipzen, A.; Xiong, Y.; et al. The regulatory and transcriptional landscape associated with carbon utilization in a filamentous fungus. *Proc. Natl. Acad. Sci. USA* **2020**, *117*, 6003–6013. [\[CrossRef\]](#) [\[PubMed\]](#)
- Xiong, Y.; Sun, J.; Glass, N.L. VIB1, a link between glucose signaling and carbon catabolite repression, is essential for plant cell wall degradation by *Neurospora crassa*. *PLoS Genet.* **2014**, *10*, e1004500. [\[CrossRef\]](#) [\[PubMed\]](#)

24. Katz, M.E.; Bernardo, S.M.; Cheetham, B.F. The interaction of induction, repression and starvation in the regulation of extracellular proteases in *Aspergillus nidulans*: Evidence for a role for CreA in the response to carbon starvation. *Curr. Genet.* **2008**, *54*, 47–55. [[CrossRef](#)]
25. Gao, Q.; Jin, K.; Ying, S.H.; Zhang, Y.; Xiao, G.; Shang, Y.; Duan, Z.; Hu, X.; Xie, X.Q.; Zhou, G.; et al. Genome sequencing and comparative transcriptomics of the model entomopathogenic fungi *Metarhizium anisopliae* and, *M. acridum*. *PLoS Genet.* **2011**, *7*, e1001264. [[CrossRef](#)]
26. Dos Reis, M.C.; Pelegrinelli Fungaro, M.H.; Delgado Duarte, R.T.; Furlaneto, L.; Furlaneto, M.C. *Agrobacterium tumefaciens*-mediated genetic transformation of the entomopathogenic fungus *Beauveria bassiana*. *J. Microbiol. Methods* **2004**, *58*, 197–202. [[CrossRef](#)]
27. Luo, S.; He, M.; Cao, Y.Q.; Xia, Y.X. The tetraspanin gene *MaPls1* contributes to virulence by affecting germination, appressorial function and enzymes for cuticle degradation in the entomopathogenic fungus, *Metarhizium acridum*. *Environ. Microbiol.* **2013**, *15*, 2966–2979. [[CrossRef](#)]
28. Liu, J.; Cao, Y.Q.; Xia, Y.X. *Mmc*, a gene involved in microcycle conidiation of the entomopathogenic fungus *Metarhizium anisopliae*. *J. Invertebr. Pathol.* **2010**, *105*, 132–138. [[CrossRef](#)]
29. Chen, X.; Liu, Y.Z.; Keyhani, N.O.; Xia, Y.X.; Cao, Y.X. The regulatory role of the transcription factor *Crz1* in stress tolerance, pathogenicity, and its target gene expression in *Metarhizium acridum*. *Appl. Microbiol. Biot.* **2017**, *101*, 5033–5043. [[CrossRef](#)]
30. Livak, K.; Schmittgen, T. Analysis of relative gene expression data using real-time quantitative PCR and the  $2^{-\Delta\Delta CT}$  Method. *Methods* **2001**, *25*, 402–408. [[CrossRef](#)]
31. Zhang, S.; Xia, Y.X.; Kim, B.; Keyhani, N.O. Two hydrophobins are involved in fungal spore coat rodlet layer assembly and each play distinct roles in surface interactions, development and pathogenesis in the entomopathogenic fungus, *Beauveria bassiana*. *Mol. Microbiol.* **2011**, *80*, 811–826. [[CrossRef](#)] [[PubMed](#)]
32. CAZy Database. Available online: <http://www.cazy.org/> (accessed on 18 March 2021).
33. Nosedal, I.; Mancera, E.; Johnson, A.D. Gene regulatory network plasticity predates a switch in function of a conserved transcription regulator. *eLife* **2017**, *6*, e23250. [[CrossRef](#)] [[PubMed](#)]
34. Borkovich, K.A.; Alex, L.A.; Yarden, O.; Freitag, M.; Turner, G.E.; Read, N.D.; Seiler, S.; Bell-Pedersen, D.; Paietta, J.; Plesofsky, N.; et al. Lessons from the genome sequence of *Neurospora crassa*: Tracing the path from genomic blueprint to multicellular organism. *Microbiol. Mol. Biol. Rev.* **2004**, *68*, 1–108. [[CrossRef](#)] [[PubMed](#)]
35. Hutchison, E.A.; Glass, N.L. Meiotic regulators *Ndt80* and *Ime2* have different roles in *Saccharomyces* and *Neurospora*. *Genetics* **2010**, *185*, 1271–1282. [[CrossRef](#)] [[PubMed](#)]
36. Katz, M.E.; Gray, K.A.; Cheetham, B.F. The *Aspergillus nidulans xprG (phoG)* gene encodes a putative transcriptional activator involved in the response to nutrient limitation. *Fungal Genet. Biol.* **2006**, *43*, 190–199. [[CrossRef](#)]
37. Katz, M.E.; Braunberger, K.; Yi, G.; Cooper, S.; Nonhebel, H.M.; Gondro, C. A p53-like transcription factor similar to *Ndt80* controls the response to nutrient stress in the filamentous fungus, *Aspergillus nidulans*. *F1000 Res.* **2013**, *2*, 72. [[CrossRef](#)] [[PubMed](#)]
38. Krohn, N.G.; Brown, N.A.; Colabardini, A.C.; Reis, T.; Savoldi, M.; Dinamarco, T.M.; Goldman, M.H.; Goldman, G.H. The *Aspergillus nidulans* ATM kinase regulates mitochondrial function, glucose uptake and the carbon starvation response. *G3 Bethesda* **2014**, *4*, 49–62. [[CrossRef](#)]
39. Lamoureux, J.S.; Glover, J.N.M. Principles of protein-DNA recognition revealed in the structural analysis of *Ndt80*-MSE DNA complexes. *Structure* **2006**, *14*, 555–565. [[CrossRef](#)]
40. Chu, S.; Herskowitz, I. Gametogenesis in yeast is regulated by a transcriptional cascade dependent on *Ndt80*. *Mol. Cell.* **1998**, *1*, 685–696. [[CrossRef](#)]
41. Hepworth, S.R.; Friesen, H.; Segall, J. *NDT80* and the meiotic recombination checkpoint regulate expression of middle sporulation-specific genes in *Saccharomyces cerevisiae*. *Mol. Cell. Biol.* **1998**, *18*, 5750–5761. [[CrossRef](#)]
42. Naseem, S.; Min, K.; Spitzer, D.; Gardin, J.; Konopka, J.B. Regulation of hyphal growth and N-acetylglucosamine catabolism by two transcription factors in *Candida albicans*. *Genetics* **2017**, *206*, 299–314. [[CrossRef](#)] [[PubMed](#)]
43. Nitsche, B.M.; Jørgensen, T.R.; Akeroyd, M.; Meyer, V.; Ram, A.F.J. The carbon starvation response of *Aspergillus niger* during submerged cultivation: Insights from the transcriptome and secretome. *BMC Genom.* **2012**, *13*, 380. [[CrossRef](#)] [[PubMed](#)]
44. Jørgensen, T.R.; Nitsche, B.M.; Lamers, G.E.; Arentshorst, M.; van den Hondel, C.A.; Ram, A.F. Transcriptomic insights into the physiology of *Aspergillus niger* approaching a specific growth rate of zero. *Appl. Environ. Microbiol.* **2010**, *76*, 5344–5355. [[CrossRef](#)] [[PubMed](#)]
45. Hopke, A.; Brown, A.J.P.; Hall, R.A.; Wheeler, R.T. Dynamic fungal cell wall architecture in stress adaptation and immune evasion. *Trends Microbiol.* **2018**, *26*, 284–295. [[CrossRef](#)] [[PubMed](#)]
46. Latgé, J.P.; Mouyna, I.; Tekaiia, F.; Baeuvais, A.; Debeaupuis, J.P.; Nierman, W. Specific molecular features in the organization and biosynthesis of the cell wall of *Aspergillus fumigatus*. *Med. Mycol.* **2005**, *43* (Suppl. 1), S15–S22. [[CrossRef](#)]
47. Rispaill, N.; Soanes, D.M.; Ant, C.; Czajkowski, R.; Grünler, A.; Huguet, R.; Perez-Nadales, E.; Poli, A.; Sartorel, E.; Valiante, V.; et al. Comparative genomics of MAP kinase and calcium-calcineurin signaling components in plant and human pathogenic fungi. *Fungal Genet. Biol.* **2009**, *46*, 287–298. [[CrossRef](#)]
48. Levin, D.E. Regulation of cell wall biogenesis in *Saccharomyces cerevisiae*: The cell wall integrity signaling pathway. *Genetics* **2011**, *189*, 1145–1175. [[CrossRef](#)]
49. Mayer, A.M.; Staples, R.C. Laccase: New functions for an old enzyme. *Phytochemistry* **2002**, *60*, 551–565. [[CrossRef](#)]



50. Pereira-Junior, R.A.; Huarte-Bonnet, C.; Paixão, F.R.S.; Roberts, D.W.; Luz, C.; Pedrini, N.; Fernandes, É.K.K. Riboflavin induces *Metarhizium* spp. to produce conidia with elevated tolerance to UV-B, and upregulates photolyases, laccases and polyketide synthases genes. *J. Appl. Microbiol.* **2018**, *125*, 159–171. [[CrossRef](#)]
51. Butt, T.M.; Coates, C.J.; Dubovskiy, I.M.; Ratcliffe, N.A. Entomopathogenic fungi: New insights into host-pathogen interactions. *Adv. Genet.* **2016**, *94*, 307–364. [[CrossRef](#)]
52. Ballester, A.R.; Marcet-Houben, M.; Levin, E.; Sela, N.; Selma-Lazaro, C.; Carmona, L.; Wisniewski, M.; Droby, S.; Gonzalez-Candela, L.; Gabaldon, T. Genome, transcriptome, and functional analyses of *Penicillium expansum* provide new insights into secondary metabolism and pathogenicity. *Mol. Plant Microbe Interact.* **2015**, *28*, 232–248. [[CrossRef](#)] [[PubMed](#)]
53. Thomas, E.; Noar, R.D.; Daub, M.E. A polyketide synthase gene cluster required for pathogenicity of *Pseudocercospora fijiensis* on banana. *PLoS ONE* **2021**, *16*, e0258981. [[CrossRef](#)] [[PubMed](#)]